applied sciences

MDPI

Article

Interface Behavior Analysis of Different Geomembrane Liner Systems Based on PIV Techniques

Junli Gao * and Jiajun Wang

School of Mechanics and Engineering Science, Shanghai University, Shanghai 200072, China; shuwjj@shu.edu.cn
* Correspondence: susan_jl@staff.shu.edu.cn

Abstract: The interfacial friction performance of the liner system has an important influence on the overall stability of modern landfills, but the interface of the liner system using conventional geomembranes may have problems such as shear failure and slip along the liner system. Accordingly, the concept of a ribbed geomembrane was proposed. Based on the laboratory model tests, the variation laws of *p*–*s* curves and the additional stress of sand were studied under different values of shape, rib spacing, and rib height. A series of particle image velocimetry (PIV) analyses of sand particles were performed to provide insight into the reinforcement mechanism of the ribbed geomembrane liner system. The results indicated that the ribbed geomembrane could obviously improve the stability of the liner system compared with the smooth geomembrane. The ribbed geomembrane formed an indirect influence area with sand in a specific range. The ribbed geomembrane with optimal values of rib spacing and rib height was beneficial to reduce the settlement of the upper sand and the stress redistribution of the sand particles.

Keywords: ribbed geomembrane; laboratory model test; particle image velocimetry (PIV); liner system; influence area

Citation: Gao, J.; Wang, J. Interface Behavior Analysis of Different Geomembrane Liner Systems Based on PIV Techniques. *Appl. Sci.* **2023**, *13*, 6614. https://doi.org/10.3390/app13116614

Academic Editor: José Manuel Moreno-Maroto

Received: 20 April 2023
Revised: 22 May 2023
Accepted: 27 May 2023
Published: 29 May 2023

1. Introduction

Landfill liner systems are generally composed of cohesive soil and geosynthetic materials (e.g., geomembranes, geotextiles, etc.). As the shear strength of the interface between geosynthetic materials is often less than the shear strength of the interface between the overlying refuse and geosynthetic materials, instability often occurs between geosynthetic materials in landfill liner systems. Therefore, the concept of the ribbed geomembrane was proposed by Gao et al. [1].

Direct shear tests and theoretical analyses of the interface between ribbed geomembranes and geotextiles have shown that ribbed geomembranes can, to a certain extent, effectively improve the frictional properties of the interface and mitigate the destabilization of the liner system. Similar structural materials such as ribbed geomembranes have also been investigated by domestic and international scholars. The theory of the indirect influence zone was proposed by Bao [2], who pointed out that the reinforcing effect of the reinforcing material would cause the soil around it to form a "reinforced soil body". Irsyam et al. [3] conducted a direct shear test on the geogrid using hot wax and obtained the shear surface and displacement vector distribution of loose sand and dense sand at different cross-rib spacing. The shear zone formation of H–V reinforced sand specimens was numerically simulated in detail by Zhang et al. [4] to reveal the progressive damage law of shear zone generation and expansion in H–V reinforced soils. Zhou et al. [5] and Yang et al. [6] investigated the reinforcement length and height of the reinforced soil foundation by indoor model tests and pointed out that the optimum reinforcement length was three times the foundation width, and the optimum number of reinforcement layers was two to three. Oda et al. [7] analyzed the generation and development of shear zones in the soil by finite element simulation of triaxial tests.

In order to study ribbed geomembranes in more depth, this paper investigates the effects of rib shape, rib spacing, and rib height on the load settlement pattern of the ribbed geomembrane–geotextile liner system and the additional stresses in the landfill sand based on preliminary direct shear tests and reinforcement theory [8,9], with the aim of providing a more comprehensive representation of the properties of the ribbed geomembrane–geotextile interface through model tests and PIV analysis techniques.

2. Laboratory Tests

2.1. Devices

As shown in Figure 1, the test devices used in this research included a model test system, a PIV system, and data acquisition systems. The model container (600 mm × 290 mm × 400 mm) was composed of a 25 mm thick steel plate welding skeleton and transparent high-strength plexiglass plates. The loading device was a dynamic triaxial apparatus (GCTS). A 200 mm × 290 mm hardwood loading board was placed in the middle of the top surface of the sand. The load was controlled at a uniform speed of 40 N/s with a controlled stress method. Due to the limitations of the loading device, the loading was terminated at 150 kPa. The test data were collected by a displacement gauge (YHD-100; range 0–50 mm) and three sand pressure cells (range 0–500 kPa). The test data were processed by the TK-ST-DA 16-channel wireless receiver, TK-ST wireless transceiver, and supporting acquisition processing software. The PIV system consisted of a charge-coupled device (CCD) camera (B5M16; 5 megapixels; image acquisition rate 11.3 frames per second) and particle image velocimetry software PIVlab 2.40.

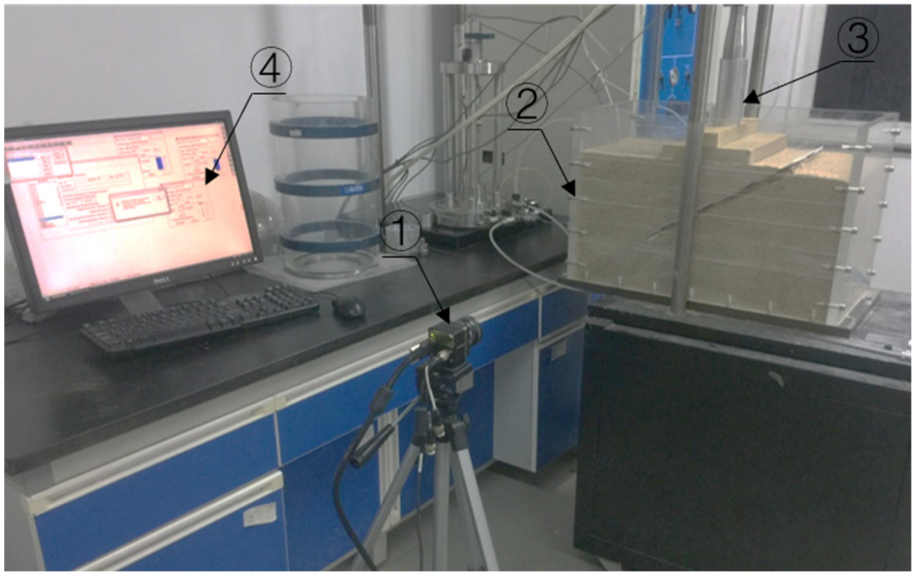

Figure 1. Model test equipment for PIV investigation. ① CCD camera; ② Model container; ③ Loading device; ④ PIV analysis software.

2.2. Materials

The specific gravity of the sand was 2.712, the water content was 1.51, the coefficient of uniformity was 2.07, and the coefficient of curvature was 0.87. The smooth geomembrane samples were made of high-density polyethylene (HDPE) with a minimum density of 0.939 g/cm^3. The size of the smooth geomembrane sample was 360 mm × 290 mm × 1.5 mm, the yield strength was 22 N/mm, and the breaking strength was 40 N/mm. The ribbed geomembrane samples were made by sticking ribs to the surface of the smooth geomembrane. In order to prevent the ribs from falling off, they were nailed to the smooth geomembrane. The size of the strip rib was 30 mm × 290 mm, and the block rib size was 30 mm × 30 mm. The layout plan is shown in Figure 2.

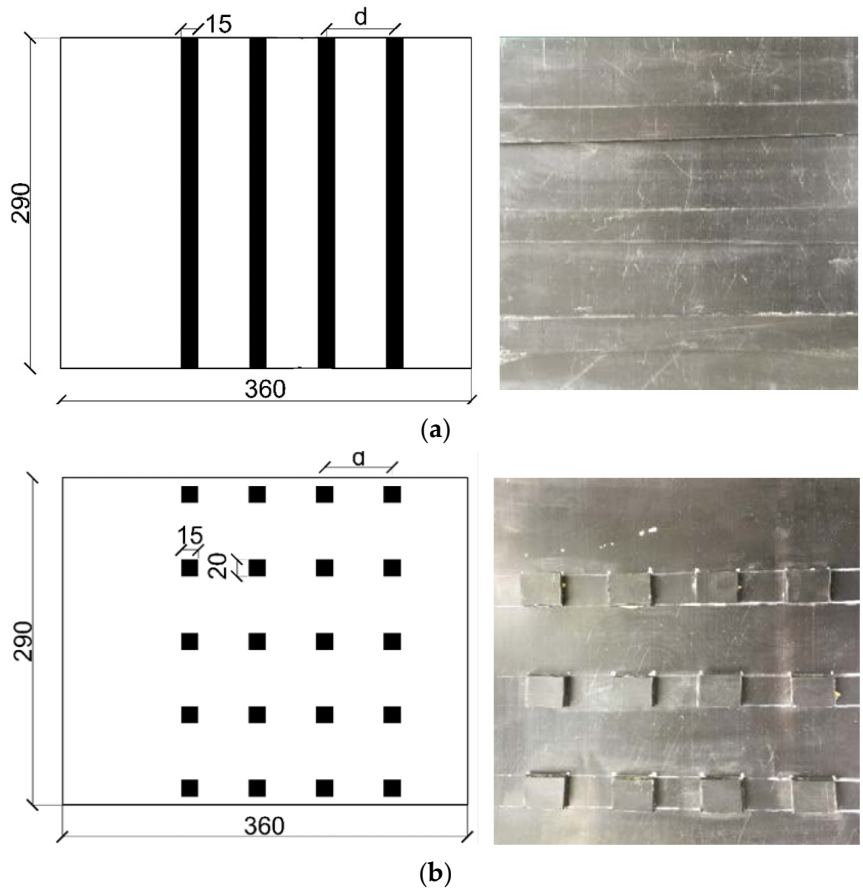

Figure 2. Layouts of ribbed geomembrane samples (unit: mm). (**a**) Strip rib. (**b**) Block rib.

A non-woven geotextile is a kind of permeable geosynthetic made of synthetic fibers by acupuncture or knitting. During the test, the non-woven geotextile was tightly attached to the geomembrane under the extrusion of the upper sand. The physical properties of the non-woven geotextile sample are shown in Table 1.

Table 1. The physical properties of the non-woven geotextile sample.

Thickness (mm)	Minimum Density (g/m^2)	Breaking Intensity (kN/m)	Puncture Resistance of CBR (kN)	Tearing Strength (kN)
3	400	12.5	2.1	0.33

2.3. Test Plan

This paper used a ribbed geomembrane–geotextile liner system to study the settlement and additional stress of landfill sand under different working conditions. The slope ratio used in the laboratory tests was 1:1.5, and the landfill height was 300 mm, as shown in Figure 3. As shown in Table 2, 19 test conditions were designed considering different rib shapes, rib spacings, and rib heights. Three parallel tests were carried out for each condition with the smooth geomembrane as a comparison.

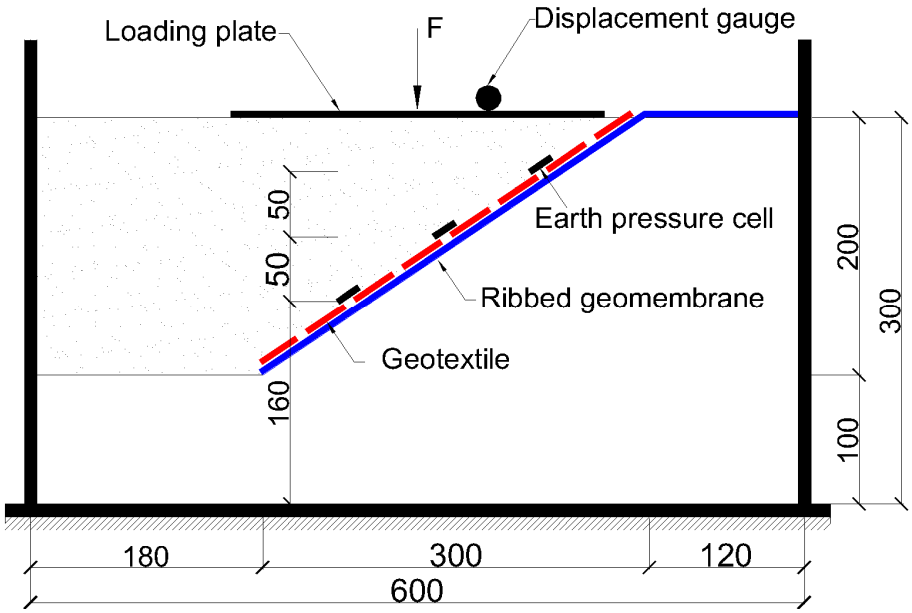

Figure 3. Model test arrangement (unit: mm).

Table 2. Test conditions.

Rib Shape	Rib Spacing *d* (mm)	Rib Height *h* (mm)
Strip rib, block rib, smooth	50, 60, 80	3, 4.5, 6

2.4. Test Procedure

The scale line and slope shape were marked on the model container before the test. The compactness of the sand was ensured to 80% during the sand filling process, and the foam board model was used to build the slope. In the process of filling sand, three sand pressure cells were embedded in the specified positions. During the filling process, the sand interface was kept flat with the scale line, and the slope surface was corrected after filling to the specified height. After that, the geomembrane and geotextile were laid on the slope foundation. Then the displacement gauge and the loading board were installed vertically, and the loading device was aligned with the center of the loading board. After connecting the sand pressure cells, the displacement gauge and wireless receiver were opened on the computer. After the model preloading was completed, the equipment was checked for normal operating. Each group of tests was completed when loading to the final load.

3. Results and Discussion

3.1. Model Settlement Analysis

The relative reduction in the settlement of the ribbed and smooth samples was calculated at the final load. The maximum load of this model test was 150 kPa. When the settlement value increased suddenly and the sand around the loading board rose laterally, the model was regarded as reaching the ultimate load. As shown in Table 3, it can be seen that the ribbed geomembrane reduced the settlement of the upper sand by 13.35–52.32% compared with the smooth geomembrane system. It was proved that the ribbed geomembrane reduced the settlement of upper sand significantly.

Table 3. Analysis of settlement under different conditions.

Test Conditions			Settlement S (mm)	Reduction Δ (%)
Rib Shape	**Rib Spacing d (mm)**	**Rib Height h (mm)**		
Smooth	/	/	5.39	/
Strip rib	50	3	3.63	35.25
		4.5	3.43	36.36
		6	3.98	26.16
	60	3	3.45	36.01
		4.5	3.11	42.30
		6	3.41	36.73
	80	3	4.25	21.15
		4.5	4.3	20.22
		6	4.45	17.44
Block rib	50	3	3.49	35.25
		4.5	3.41	36.73
		6	4.01	25.60
	60	3	3.18	41.00
		4.5	2.57	52.32
		6	3.66	32.09
	80	3	4.32	19.85
		4.5	4.05	24.86
		6	4.67	13.35

Note: The reduction in the model settlement of the ribbed geomembrane relative to that of the smooth geomembrane was calculated as $\Delta = |S_{Rib} - S_{Smooth}| / S_{Smooth} \times 100\%$.

3.2. Model p–s Curve Analysis

The *p–s* curves under different rib shapes, rib spacings *d*, and rib heights *h* were analyzed in this section. The *p–s* curves of the strip and block ribbed geomembrane were similar to the variation of rib spacings and rib heights. Therefore, the following section focuses on analyzing the *p–s* curves of block ribbed geomembranes under different rib spacings *d* and rib heights *h*.

Figure 4 shows the effect of different rib shapes on the *p–s* curve. From Figure 4a–c, it can be seen that the ribbed geomembrane effectively reduced the settlement of the liner system model compared with the smooth geomembrane. In addition, the settlement of the strip ribbed geomembrane liner system was smaller than that of the block ribbed geomembrane liner system in each working condition. The settlement difference was maximum at d = 60 mm. On one hand, compared with block rib, strip rib had a larger friction force when sliding with the soil, as well as a more robust extrusion and occlusal effect, thus providing a more significant passive impedance force. On the other hand, the end-bearing resistance of ribs increased the overall stiffness of the surrounding soil to a greater extent and then reduced the settlement.

As shown in Figure 5, when the rib spacing increased from 50 to 60 mm, the settlement of corresponding rib height h = 3 mm, 4.5 mm, and 6 mm decreased by 8.88%, 24.63%, and 8.73%, respectively. It could be seen that when the rib height was too high, the reinforcement mechanism would be weakened. The reason was the rib height made the geomembrane bond too closely with the soil above it, resulting in a shear plane at the lower edge of the geomembrane, thus increasing the settlement. When the rib spacing was further increased to 80 mm, the corresponding settlement increased by 35.8, 57.57, and 27.04%. It could be seen that when the rib spacing was too high, it also had the opposite effect, which was directly caused by weakening the stiffening mechanism.

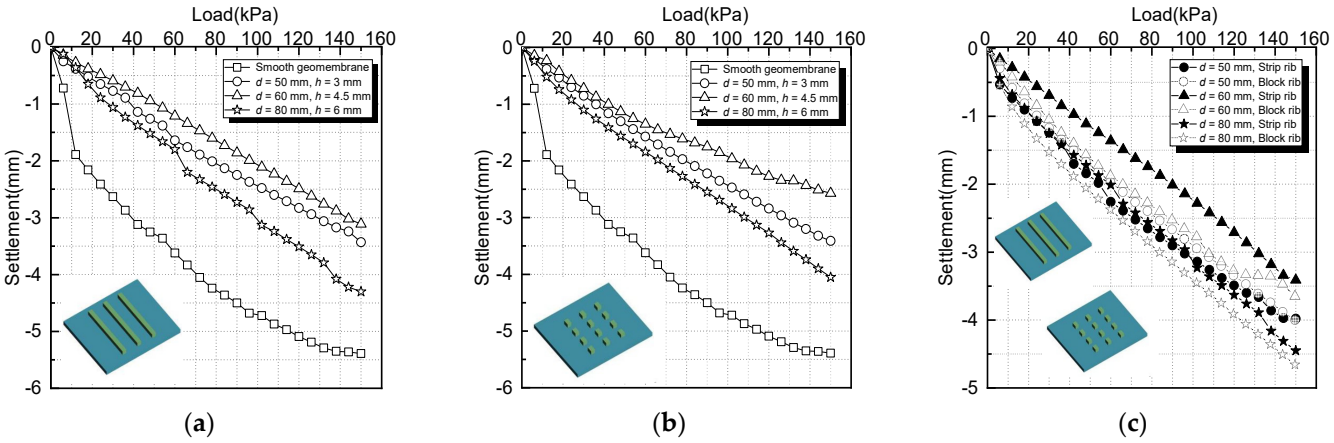

Figure 4. Effect of rib shapes on *p*–*s* curves. (**a**) Smooth and strip rib. (**b**) Smooth and block rib. (**c**) Strip and block rib.

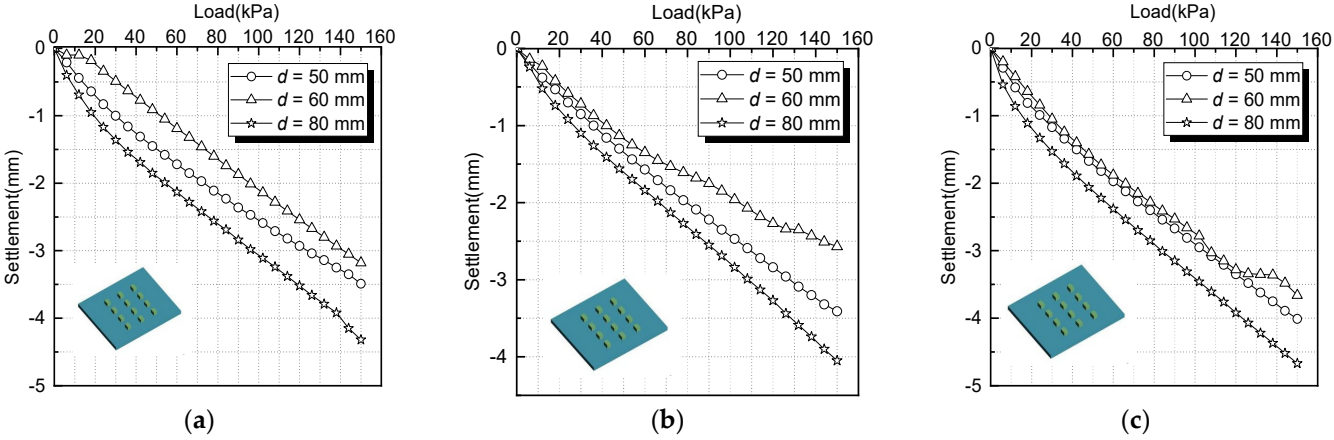

Figure 5. Influence of rib spacing on *p*–*s* curves. (**a**) h = 3 mm. (**b**) h = 4.5 mm. (**c**) h = 6 mm.

The above test results show that the rib shapes, rib spacings d, and rib heights h directly affected the reinforcing effect of the ribbed geomembrane on the sand. Within a specific range, the influence of the rib shapes was inconspicuous when the rib spacing was small, and the settlement of the strip ribbed geomembrane liner system decreased with the increase in the rib spacing. The friction and interlocking forces of the ribs on the sand increased with the increase in the rib spacing d and rib height h. However, the complex formed by the ribs and the surrounding sand exceeded the limit value for the reinforcing effect of the ribs. After exceeding the limit value, the reinforcing effect of bearing resistance on the sand was weakened. The formation range of the composite was reduced, resulting in decreased overall stability and bearing capacity.

3.3. Additional Stress Analysis of Sand

The additional stress is the incremental stress caused by the load in the foundation. It is the main cause of deformation due to the loss of stability of the foundation.

The additional stress distribution of the smooth geomembrane model is shown in Figure 6. From Figure 6, it can be seen that the additional stress of the sand in the smooth geomembrane liner system gradually decreased from the top to the bottom, indicating that the upper load was transmitted downward. The attenuation of the upper load was consistent with the law that the additional stress in the sand decreases with the increase in the buried depth [10].

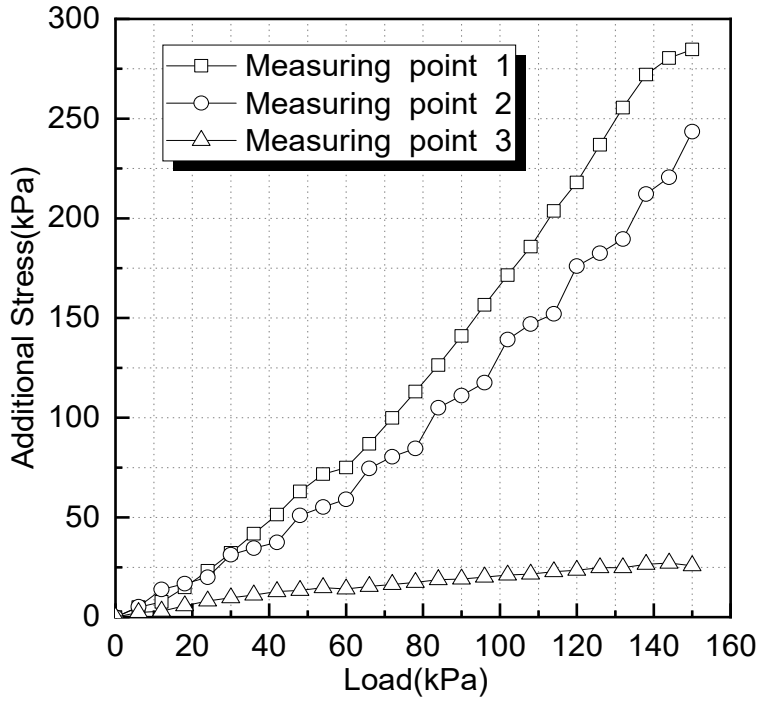

Figure 6. Additional stress distributions of the smooth geomembrane model.

The additional stress distribution of the ribbed geomembrane model is shown in Figure 7. From Figure 7, it can be seen that the additional stress of the sand in the ribbed geomembrane liner system decreased uniformly from top to bottom, indicating that the ribs affected the distribution of additional stress in the sand during the downward transfer of upper load. It can be seen that the additional stress of the model decreased from top to bottom, which accorded with the law of load transfer in the model. Compared with the smooth geomembrane condition, the additional stress of the ribbed geomembrane model was uniform. This was because the ribs produced a vertical component force under the upper load, which could offset the upper load to reduce the load. It made the internal stress distribution of the model change so that the upper load was partly transferred to the bottom. When the ribbed geomembrane liner system was subjected to the upper load, part of the upper load was offset by the vertical upward force generated by the ribs. This changed the additional stress distribution of the sand and avoided the overall instability or reduction of the bearing capacity of the model.

Taking the rib height h = 6 mm as an example to analyze the effect of the rib spacing d on the additional stress distribution of the block ribbed geomembrane model (Figure 8), compared with rib spacings of d = 50 mm and 80 mm, the additional stress of the sand at measuring points 1 and 2 was significantly lower when d = 60 mm. The additional stress of the sand at measuring point 3 and the additional stress of the sand with rib spacing d = 60 mm were significantly higher than those of other conditions. This showed that when the rib spacing d = 60 mm, the ribs blocked the downward movement of sand, reduced the tensile stress on the geomembrane when sand slipped, and improved the overall stability model. When the rib spacing d = 80 mm, the additional stress of measuring point 3 and measuring point 2 at the final load were almost the same. This showed that when the rib spacing exceeded a specific value, the overall stability of the model may be destroyed. It was also indicated that there was an optimal value for the rib spacing of the ribbed geomembrane.

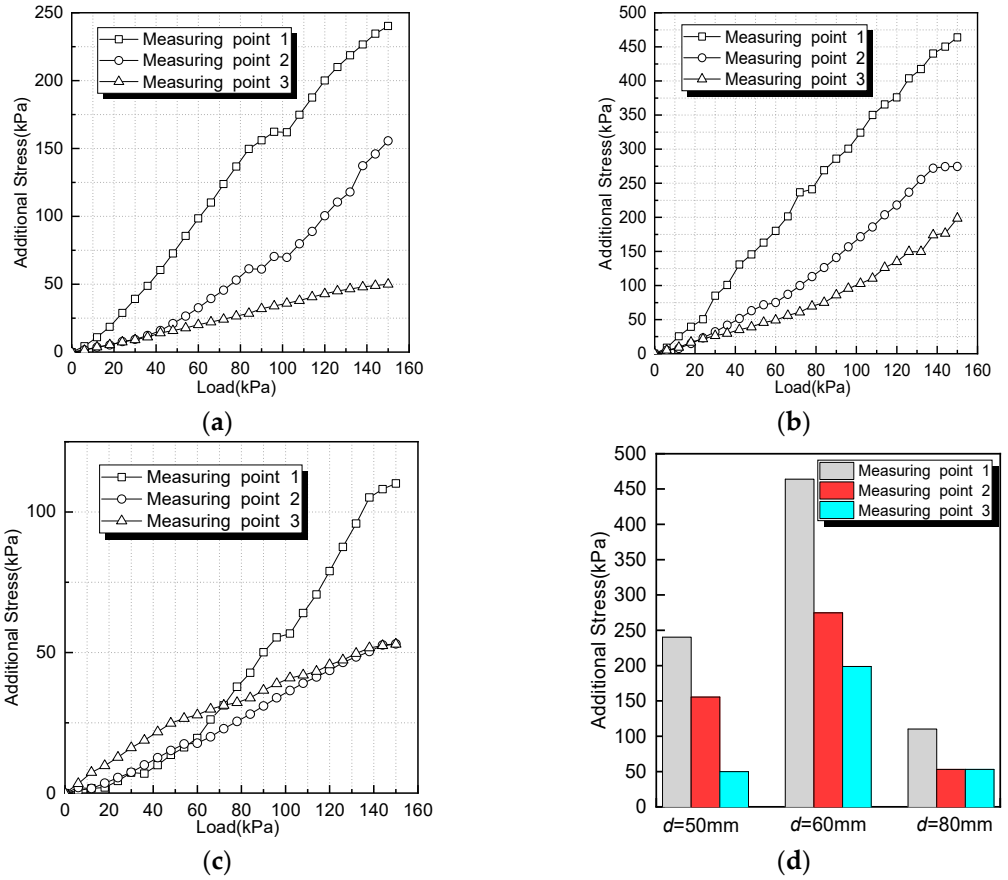

Figure 7. Distribution of additional stress in the block rib geomembrane model. (**a**) d = 50 mm, h = 4.5 mm. (**b**) d = 60 mm, h = 4.5 mm. (**c**) d = 80 mm, h = 4.5 mm. (**d**) p = 150 kPa, h = 4.5 mm.

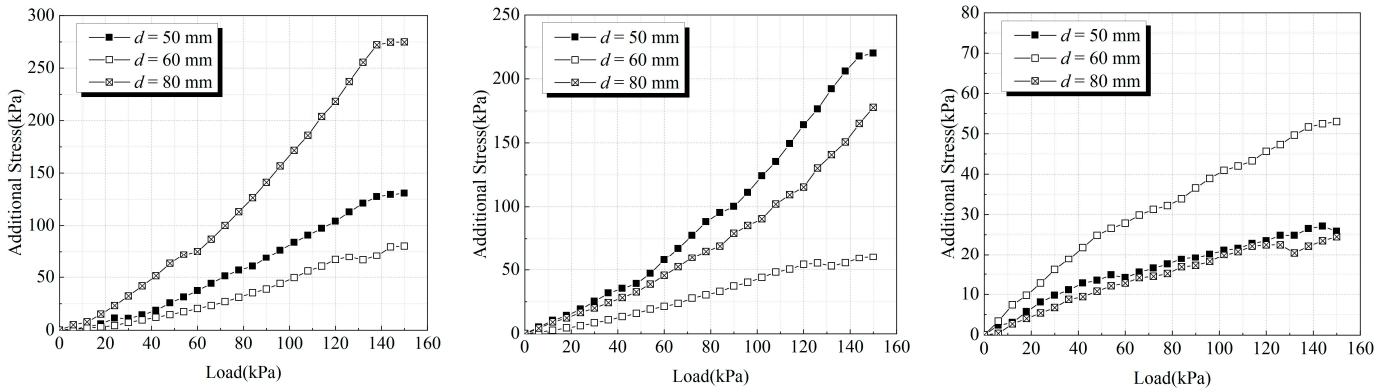

(**a**) Measuring point 1 (**b**) Measuring point 2 (**c**) Measuring point 3

Figure 8. Influence of rib spacing on the additional stress of sand.

Due to the similar effects of different rib heights on the additional stress of the sand, 80 mm rib spacing conditions were used as an example to analyze the additional stress distribution of rib height on the ribbed geomembrane model. As shown in Figure 9, it can be seen from the figure that when the rib height h = 3 mm, the values at measuring points 1 to 3 varied reached maximums. The additional stress of the sand at different measurement points decreased with the increase in the landfill depth. When the rib height h = 4.5 mm, from measuring points 1 to 3, there was additional stress of the sand with the increase in the landfill depth. The overall change trends were relatively stable, which showed that the blocks played an active role in bearing the blockage of sand movement. When the

rib height h = 6 mm, the additional stress of the sand was about 270 kPa at measuring point 1 and about 30 kPa at measuring point 3. The effect was slightly better than with the rib height h = 3 mm but was still inferior to that with h = 4.5 mm. This showed that the inappropriate values of h may weaken the reinforcing effect of the ribs. The optimal rib height could strengthen the reinforcing effect, increase the end-resistance of the ribs, and enhance the interaction between the ribbed geomembrane and the sand. It can be concluded that the optimal rib height was beneficial to the redistribution of the additional stress of the sand.

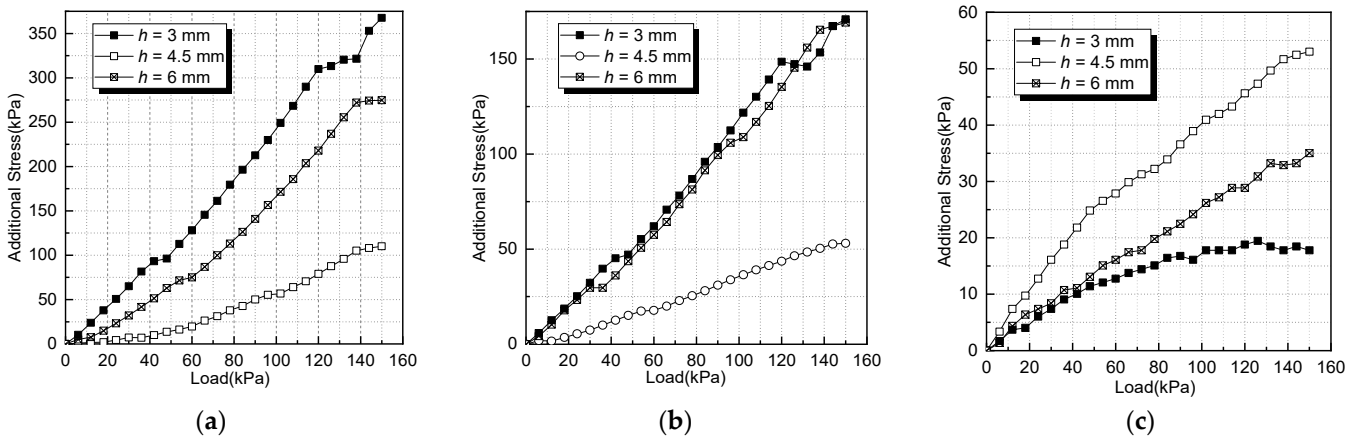

Figure 9. Influence of rib height on the additional stress of sand. (**a**) Measuring point 1. (**b**) Measuring point 2. (**c**) Measuring point 3.

3.4. PIV Image Analysis

The whole process of the sand particle displacement recorded by this research provided suitable conditions for analyzing the liner system model deformation. Since the blocks were not set along the edge, the displacement of sand particles can hardly be observed. Thus, the analysis focused on the conditions of the smooth geomembrane and the strip ribbed geomembrane.

Figures 10 and 11 show the sand movement under the conditions of the smooth geomembrane and the strip ribbed geomembrane. The sand particles indicated in the figure reflected the movement trends of some particles around. In the figure, 1–4 are sand particles located in four different positions. Under the conditions of smooth geomembrane, sand particles 1 and 2 moved vertically downward, sand particle 3 deflected down to the left, and sand particle 4 deflected down to the right. Under the conditions of ribbed geomembrane, sand particle 1 deflected down to the left, sand particles 2 and 3 slid downward along the interface, and sand particle 4 deflected down to the right. Due to the lower upper load, the sand particles under the loading board gradually experienced vertical downward displacements in the initial stage. When t = 2~4 s, the sand particles between the loading board and geomembrane moved down to the left, and the influence scope of the upper load increased. When t = 4~6 s, due to the limitation of the geomembrane interface, the displacements of the sand particles under the loading board gradually formed a circular slip surface. When t = 6~10 s, the displacements of the sand particles near the ribs were relatively low, but the displacements of the sand particles on the observation surface increased significantly. At this time, the range of the sliding surface expanded, and the sand particles overflowed to both sides of the loading board.

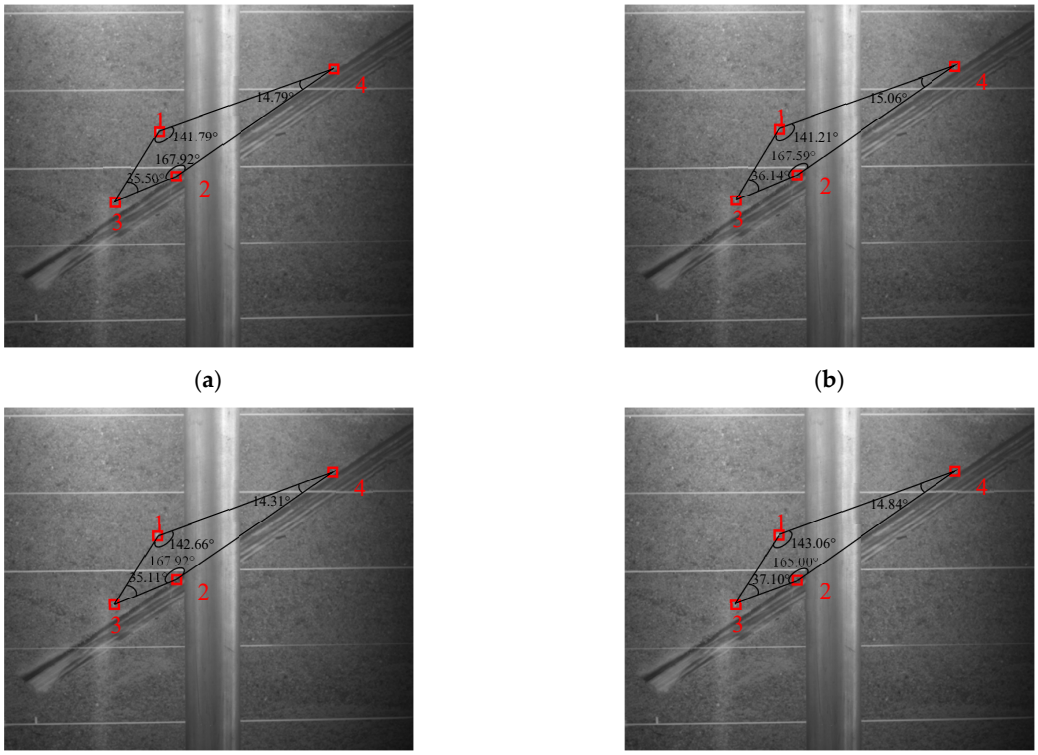

(**a**) (**b**)

(**c**) (**d**)

Figure 10. Schematic diagram of the sand movement under the conditions of the smooth geomembrane. (**a**) t = 2 s. (**b**) t = 4 s. (**c**) t = 6 s. (**d**) t = 10 s.

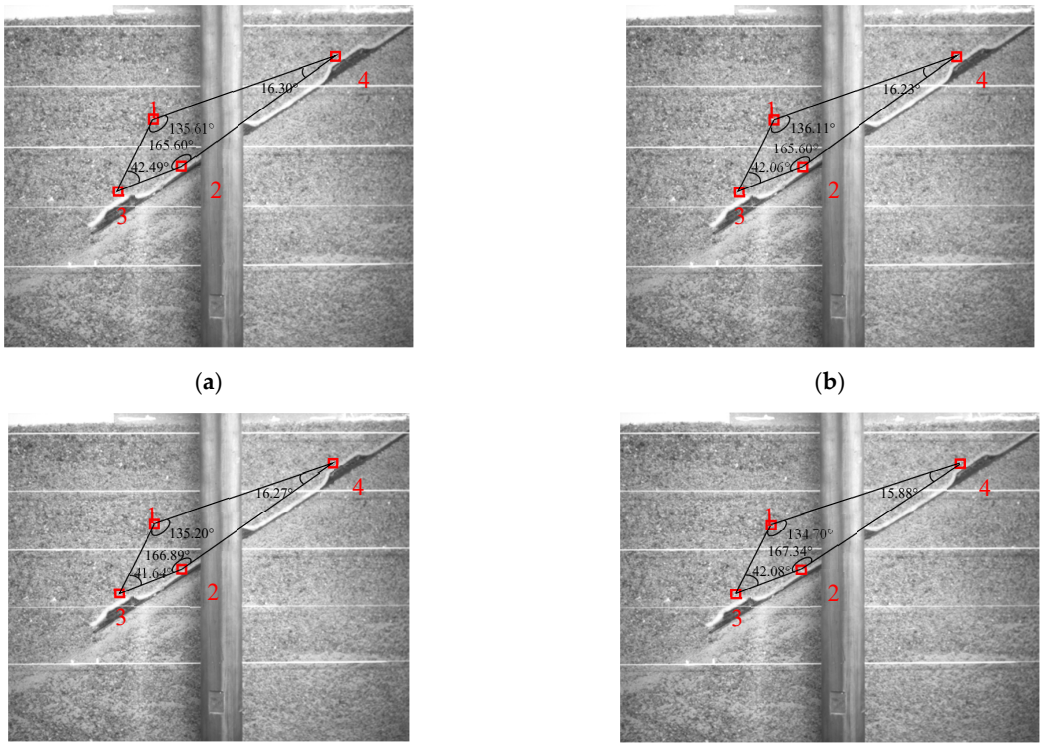

(**a**) (**b**)

(**c**) (**d**)

Figure 11. Schematic diagram of the sand movement under the conditions of the ribbed geomembrane. (**a**) t = 2 s. (**b**) t = 4 s. (**c**) t = 6 s. (**d**) t = 10 s.

3.5. Sand Displacements Analysis of Different Geomembranes

The photos of the smooth geomembrane and the ribbed geomembrane during the loading process were intercepted and calibrated, respectively, and then the cross-correlation calculation was carried out with the initial time to obtain the displacement nephogram at the corresponding time. To study the effect of ribs on the sand displacements, the horizontal and vertical displacement nephograms of the smooth geomembrane conditions were compared with the strip rib geomembrane conditions, as shown in Figures 12 and 13. The shadows in the middle of the figures were caused by the test equipment blocking 3the model container in the shooting direction. Its influence on the calculation result was eliminated by drawing masks in the PIV image settings. Figure 12 shows that the absolute value of the horizontal displacement of sand above the smooth geomembrane interface was 0.0825 mm. The absolute value of the horizontal displacement of sand above the ribbed geomembrane interface was 0.0063. As shown in Figure 13, the absolute value of the horizontal displacement of sand above the smooth geomembrane interface was 0.2275 mm, and the absolute value of the horizontal displacement of sand above the ribbed geomembrane interface was 0.0588 mm. This showed that the ribbed geomembrane reduced the horizontal and vertical displacements effectively.

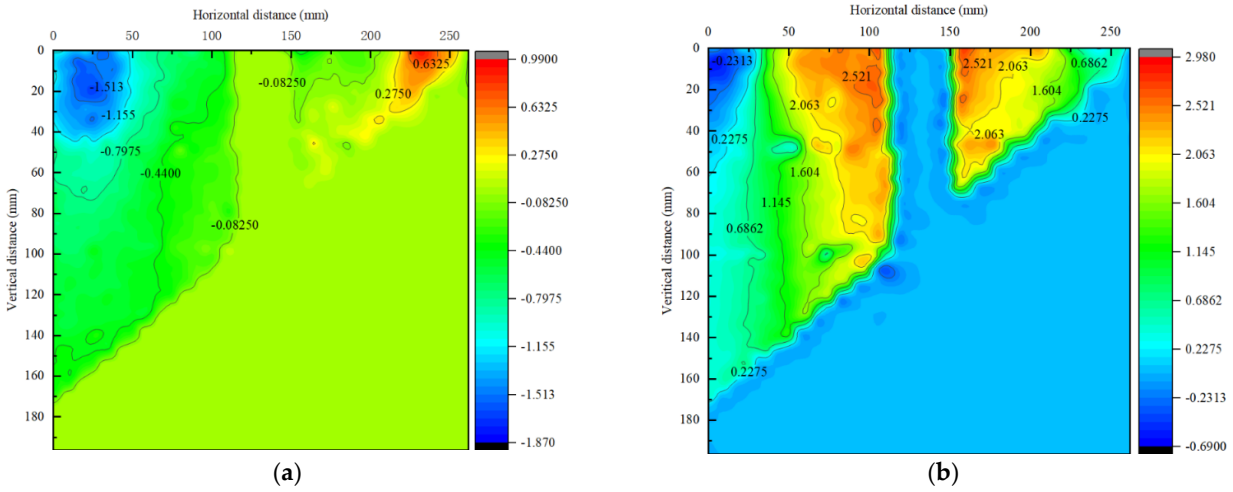

(**a**) (**b**)

Figure 12. Displacement nephograms of the smooth geomembrane condition. (**a**) Horizontal displacement. (**b**) Vertical displacement.

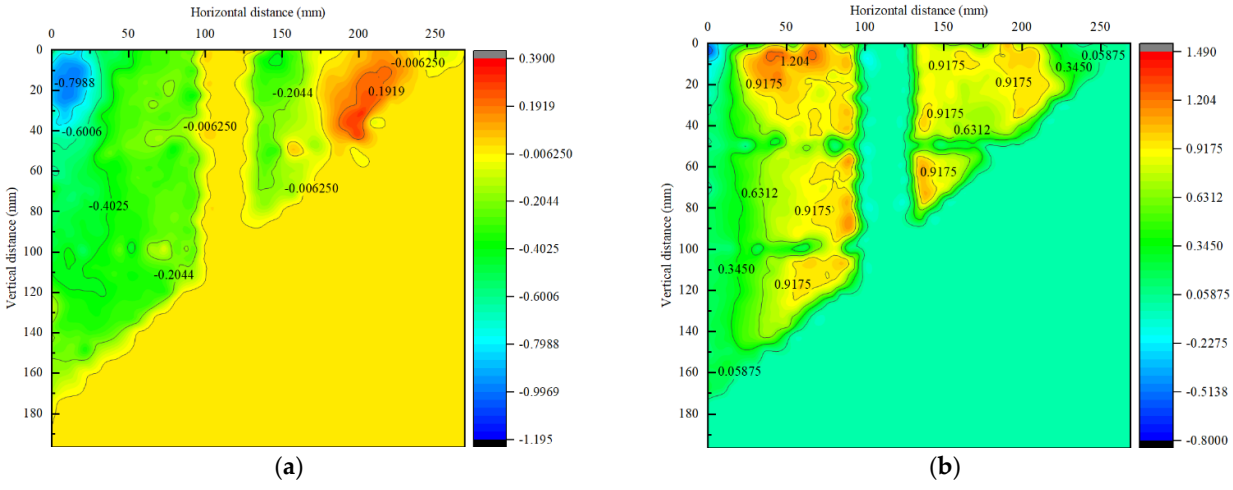

(**a**) (**b**)

Figure 13. Displacement nephograms of the ribbed geomembrane condition (d = 60 mm, h = 4.5 mm). (**a**) Horizontal displacement. (**b**) Vertical displacement.

To analyze the displacements of the sand particles above the geomembrane interface, the data in the loading process were extracted and plotted, as shown in Figures 14 and 15. It was shown that the ribs directly resisted the sand particles, formed a more comprehensive range of indirectly affected areas, and combined the sand closely. This area prevented the interface of the geomembrane liner system from slipping and constrained the deformation of the liner system. This was a kind of quasi-cohesive force, which improved the strength of the slope surface. With the increasing normal stress of the ribs, the bearing resistance of the ribs enhanced the interface shear strength significantly. At the same time, the friction resistance of the ribs increasing with the incremental upper load. Therefore, compared with the smooth geomembrane conditions, the ribbed geomembrane conditions could effectively improve the stability of the liner system, which was in accordance with the interaction mechanism between the sand and the denti-strip [11].

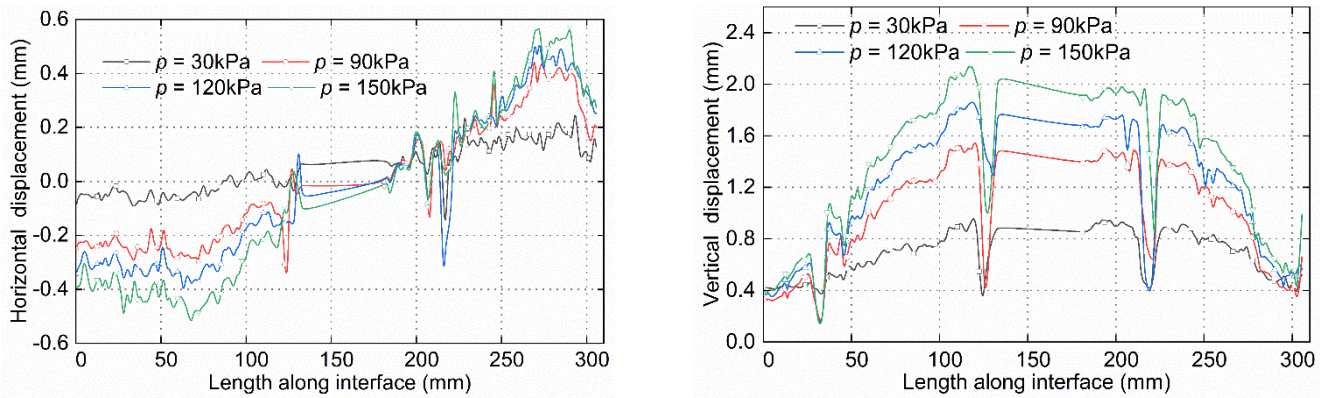

(**a**) (**b**)

Figure 14. Displacement of sand above the smooth geomembrane interface. (**a**) Horizontal displacement. (**b**) Vertical displacement.

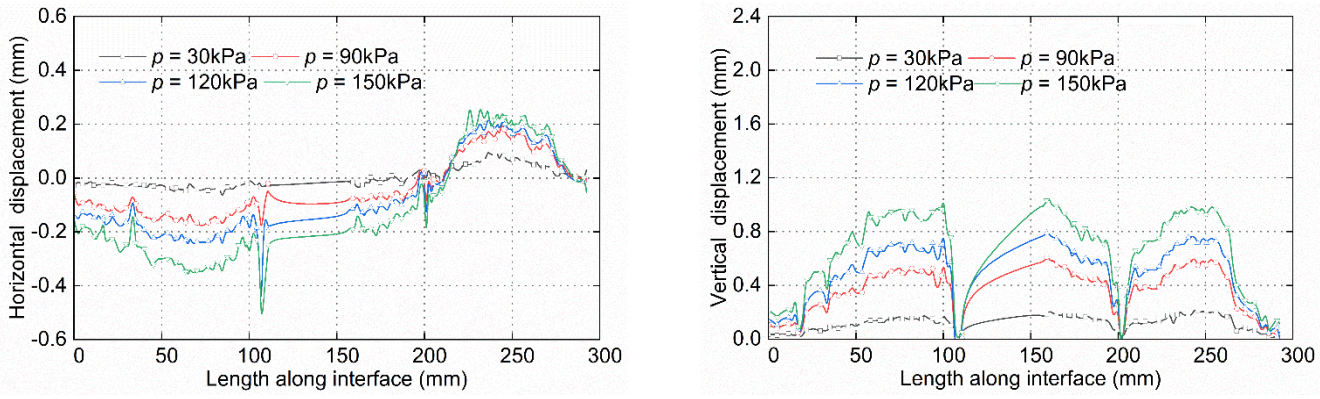

(**a**) (**b**)

Figure 15. Displacement of sand above the ribbed geomembrane interface. (**a**) Horizontal displacement. (**b**) Vertical displacement.

3.6. Analysis of Rib Spacing on Sand Displacements

Figures 16 and 17 show the horizontal and vertical displacements of different rib spacings. Compared with Figure 13, it was found that the absolute values of the sand horizontal displacement above the geomembrane interface of three working conditions (rib spacing d = 50 mm, d = 60 mm, and d = 80 mm) were 0.1625, 0.0063, and 0.1975 mm, respectively. At the same time, the absolute values of the sand vertical displacement above the geomembrane interface of the three working conditions (rib spacing d = 50 mm, d = 60 mm, and d = 80 mm) were 0.4525, 0.0588, and 0.3650 mm, respectively. This was due

to the better effect of the 60 mm rib spacing on the cohesion of sand particles around the ribs. The interaction between the ribs and the sand was not evident under the condition of 50 mm rib spacing. The reinforcing effect of the ribs on the surrounding sand was weakened under 80 mm rib spacing.

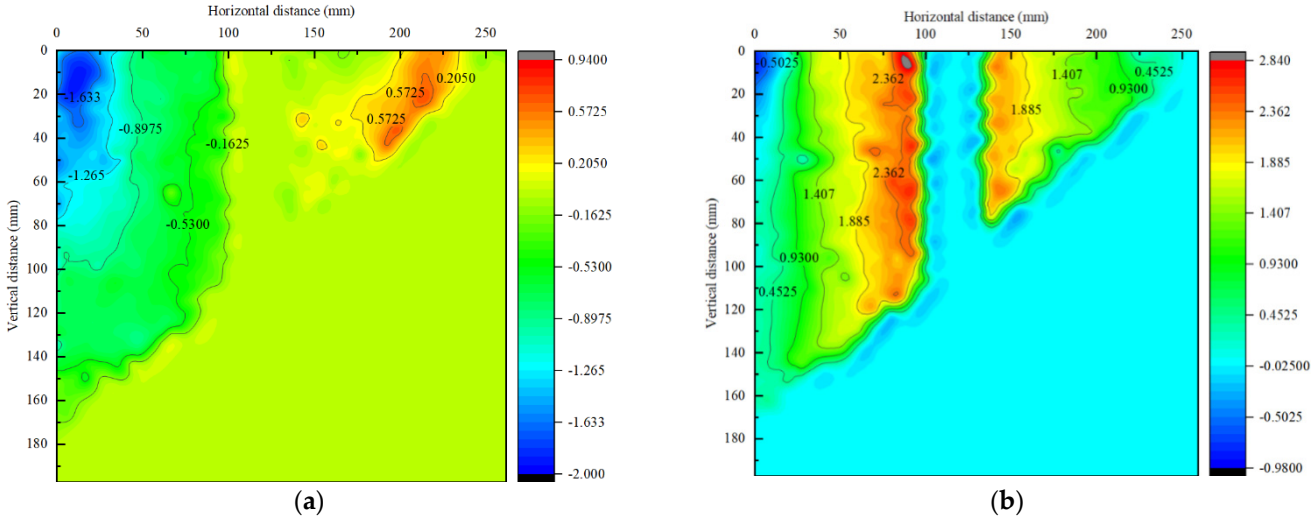

Figure 16. Displacement nephograms of smooth geomembrane conditions (d = 50 mm, h = 4.5 mm). (**a**) Horizontal displacement. (**b**) Vertical displacement.

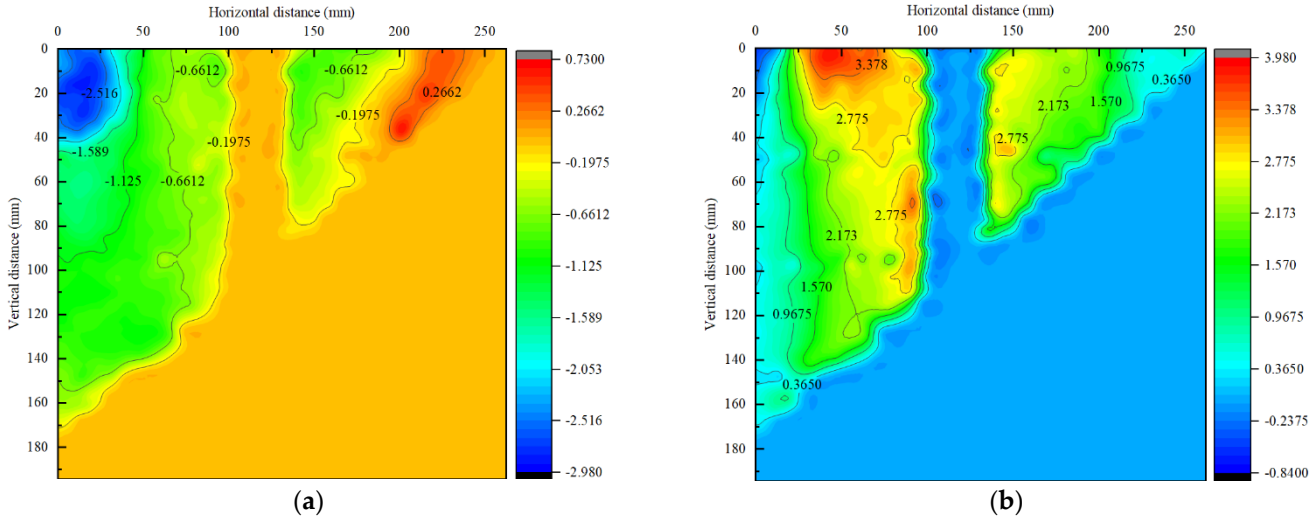

Figure 17. Displacement nephograms of ribbed geomembrane conditions (d = 80 mm, h = 4.5 mm). (**a**) Horizontal displacement. (**b**) Vertical displacement.

As shown in Figures 18 and 19, the sand displacements of different rib spacings were analyzed. Combined with Figure 15, the results showed that the horizontal and vertical displacements of the sand particles above the geomembrane interface were smaller when the rib spacing d = 60 mm. It could indicate that the 60 mm rib spacing blocked and interlocked the movements of the surrounding sand particles. It proved the optimal rib spacing of the ribbed geomembrane existed, and this was consistent with the previous experimental results.

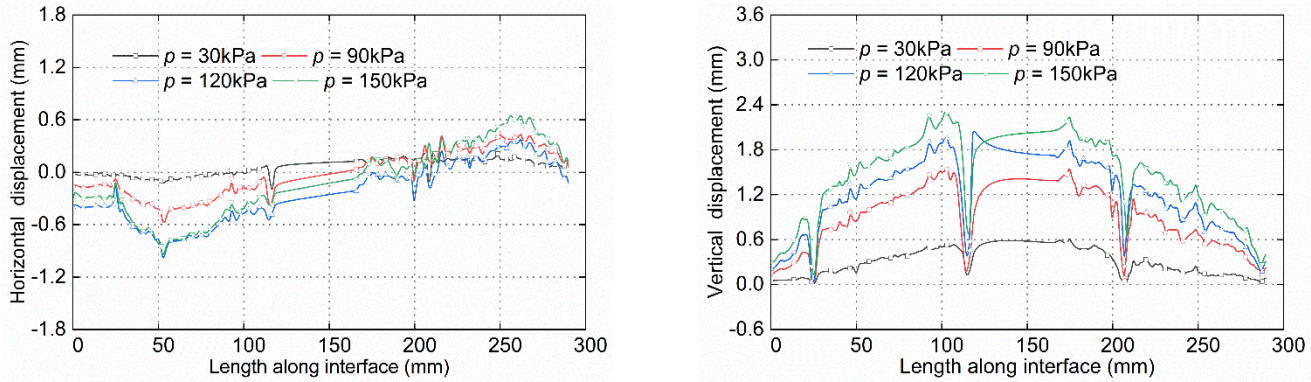

(**a**) (**b**)

Figure 18. Displacement of sand above ribbed geomembrane conditions (d = 50 mm, h = 4.5 mm). (**a**) Horizontal displacement. (**b**) Vertical displacement.

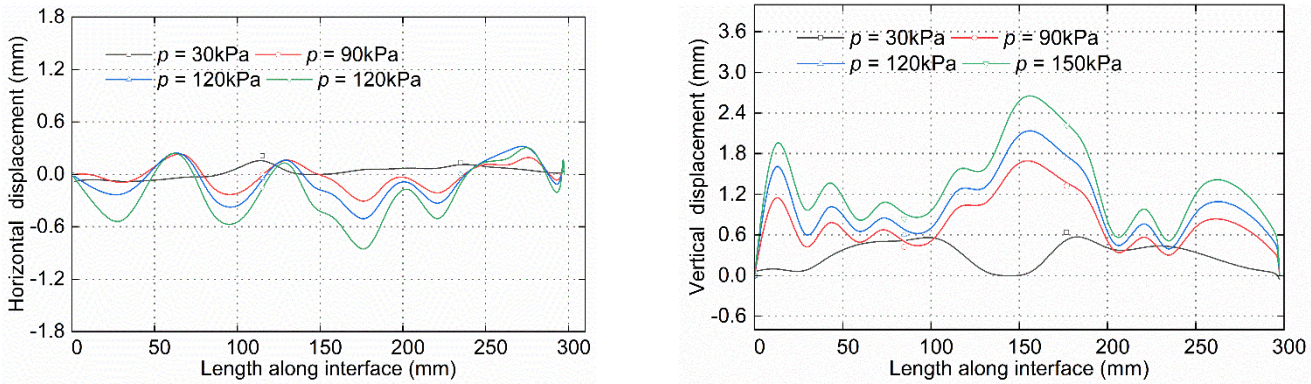

(**a**) (**b**)

Figure 19. Displacement of sand above ribbed geomembrane conditions (d = 80 mm, h = 4.5 mm). (**a**) Horizontal displacement. (**b**) Vertical displacement.

3.7. Analysis of Rib Height on Sand Displacements

Figures 20 and 21 show the horizontal and vertical displacements of different rib heights. Compared with Figure 13, it was found that the absolute values of the sand horizontal displacement above the geomembrane interface of three working conditions (rib height h = 3 mm, h = 4.5 mm, and h = 6 mm) were 0.0500, 0.0063, and 0.0725 mm, respectively. At the same time, the absolute values of sand vertical displacement above the geomembrane interface of the three working conditions (rib height h = 3 mm, h = 4.5 mm, and h = 6 mm) were 0.1200, 0.0588, and 0.0625 mm, respectively. This was because the elastic modulus of the sand increased more in the indirect influence area created by the 4.5 mm rib height, which inhibited the movement trend of the sand particles. The interaction between the ribs and the sand was small when the rib height was 3 mm, and the reinforcing effect of the ribs on surrounding sand declined when the rib height was 4.5 mm.

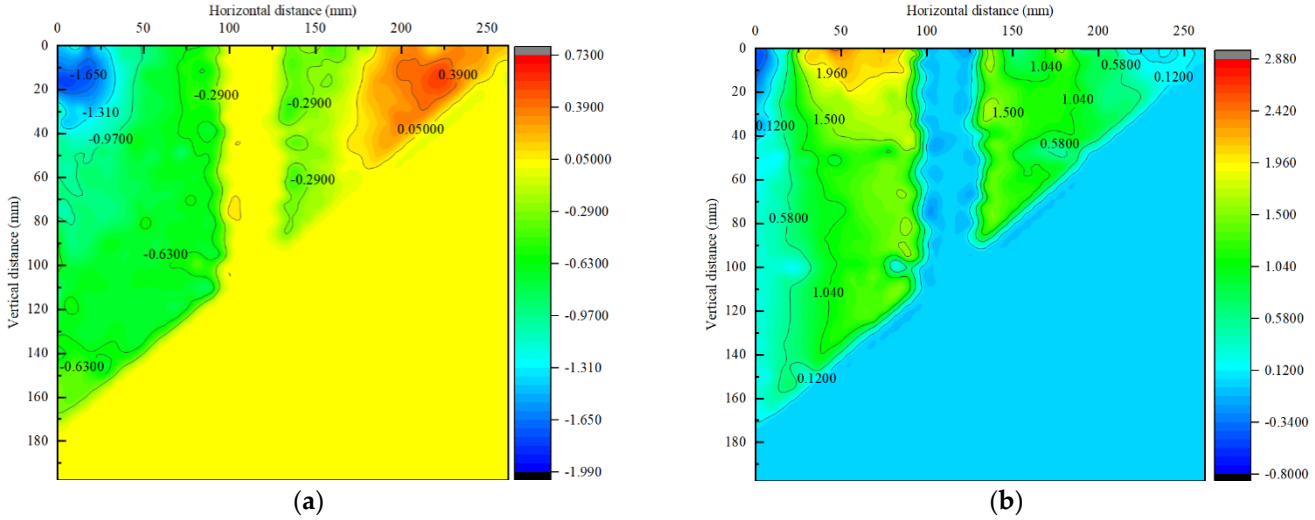

(**a**) (**b**)

Figure 20. Displacement nephograms of smooth geomembrane conditions (d = 60 mm, h = 3 mm). (**a**) Horizontal displacement. (**b**) Vertical displacement.

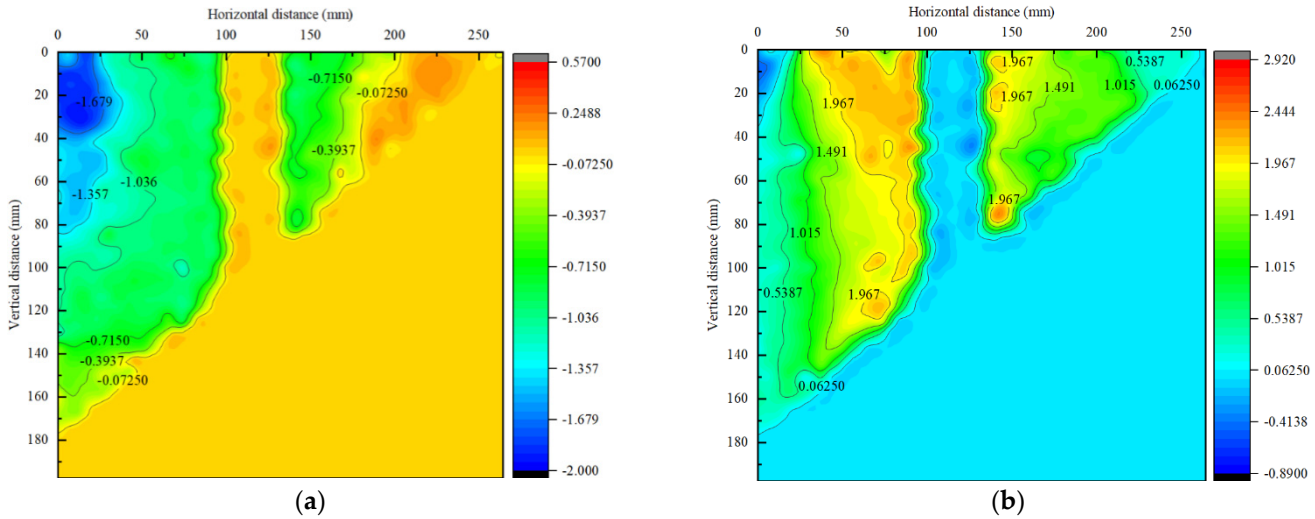

(**a**) (**b**)

Figure 21. Displacement nephograms of ribbed geomembrane conditions (d = 60 mm, h = 6 mm). (**a**) Horizontal displacement. (**b**) Vertical displacement.

As shown in Figures 22 and 23, the sand displacements of different rib heights were analyzed. Compared with Figure 15, the results showed that the horizontal and vertical displacements of the sand particles above the geomembrane interface were smaller when the rib height h = 4.5 mm. It can be concluded that the 4.5 mm rib height limited the surrounding sand particles and reduced the risk of liner system interface sliding. It verified the optimal rib height of the ribbed geomembrane, which was the same as the previous experimental results.

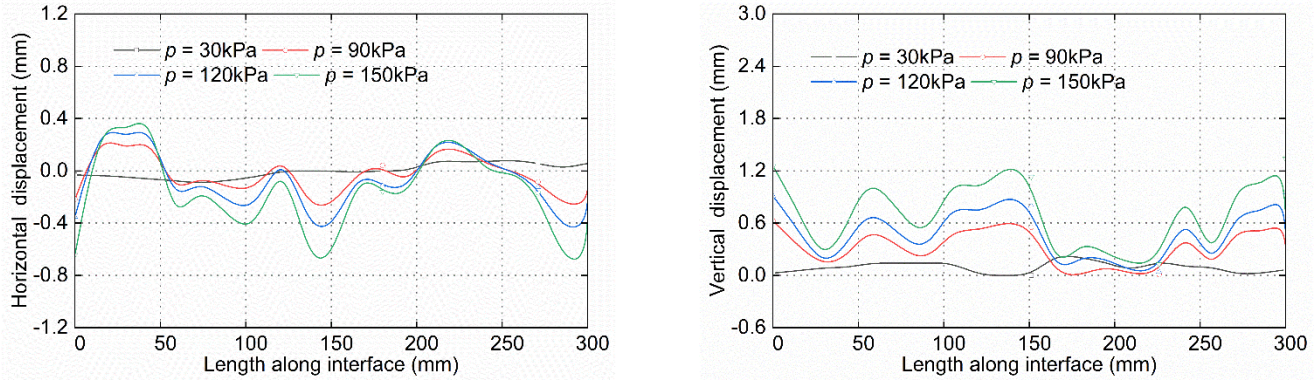

(**a**) (**b**)

Figure 22. Displacement of sand above ribbed geomembrane conditions (d = 60 mm, h = 3 mm). (**a**) Horizontal displacement. (**b**) Vertical displacement.

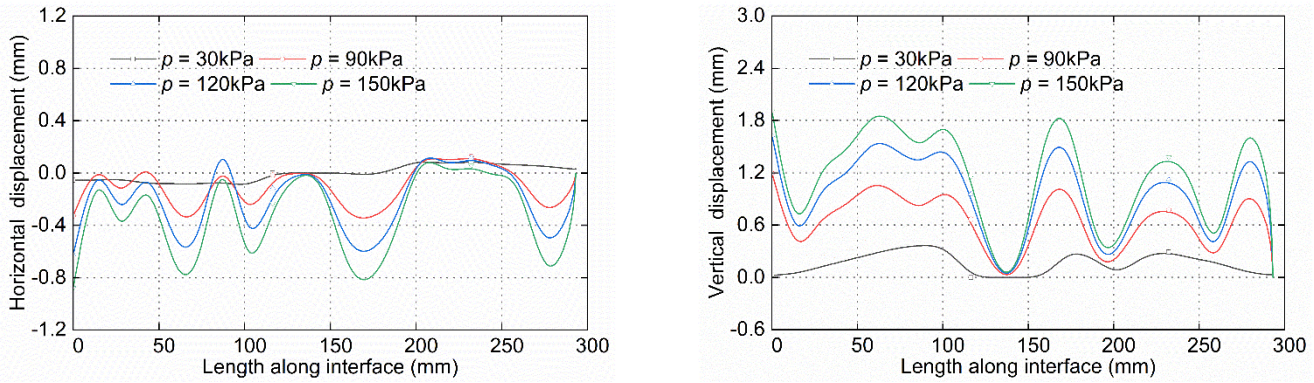

(**a**) (**b**)

Figure 23. Displacement of sand above ribbed geomembrane conditions (d = 60 mm, h = 6 mm). (**a**) Horizontal displacement. (**b**) Vertical displacement.

4. Conclusions

1. It can be seen from the comparative analysis of working conditions that the settlement of the ribbed geomembrane was significantly less than that of the smooth geomembrane. It was proved that the ribs enhanced the stability of the liner system.
2. According to the analysis of the test results, there was an optimum value of 60 mm for the rib spacing and 4.5 mm for the rib height. When the value was less than the optimal value, the ribbed geomembrane could not effectively improve the stability of the liner system. When the value was more than the optimal value, the reinforcing effect of the ribbed geomembrane on the sand gradually decreased.
3. By analyzing the additional stress of the sand, it can be concluded that the ribbed geomembrane was beneficial to the stress redistribution, thereby improving the overall stability of the liner system.
4. According to the PIV image analysis, the ribbed geomembrane can form an indirect influence area with the sand within a specific range to restrain the displacement of nearby sand particles. The indirect influence area was conducive to the stability of the liner system.

5. Prospect

This paper effectively demonstrated the advantages of a ribbed geomembrane and geotextile liner system using indoor model tests and PIV image velocimetry techniques. The results of this thesis can provide a theoretical basis for practical applications in projects such as landfills.

Author Contributions: Conceptualization, J.G.; Investigation, J.G.; Data curation, J.W.; Writing—original draft, J.G.; Writing—review & editing, J.W.; Project administration, J.G. All authors have read and agreed to the published version of the manuscript.

Funding: This research received no external funding.

Institutional Review Board Statement: Not applicable.

Informed Consent Statement: Not applicable.

Data Availability Statement: The data that support the findings of this study are available from the corresponding author, upon reasonable request.

Conflicts of Interest: The authors declare no conflict of interest.

References

1. Gao, J.L.; Zhang, M.X.; Zhang, W.J. Interface property between sand and reinforced geomembrane. *Rock Soil Mech.* **2011**, *32*, 3220–3230.
2. Bao, C.G. Study on interface behavior of geosynthetics and soil. *Chin. J. Rock Mech. Eng.* **2006**, *25*, 1735–1744.
3. Irsyam, M.; Hryciw, R.D. Friction and passive Resistance in soil reinforced by plane ribbed Inclusions. *Géotechnique* **1991**, *41*, 485–498. [CrossRef]
4. Zhang, M.X.; Zhang, S.L. Behaviour of soil reinforced with H-V inclusions by PFC^2D. *Chin. J. Geotech. Eng.* **2008**, *30*, 625–631.
5. Zhou, J.; Kong, X.L.; Wang, X.C. Bearing capacity behaviours and failure modes of reinforced grounds. *Chin. J. Geotech. Eng.* **2008**, *30*, 1265–1269.
6. Yang, Q.; Zhang, K.; Lua, M.T. Study of model test on performance of soil foundation reinforced by geogrids. *J. Dalian Univ. Technol.* **2006**, *46*, 390–394.
7. Oda, M.; Nemat-Naaser, S.; Konish, J. Stress-induced anisotropy in granular masses. *Soil Found.* **1985**, *25*, 85–97. [CrossRef] [PubMed]
8. Gao, J.L.; Zhang, M.X.; Zhang, W.J. Interface Frictional Property Between Sand and Geomembrane. In *Advances in Environmental Geotechnics, Proceedings of the International Symposium on Geoenvironmental Engineering, Hangzhou, China, 8–10 September 2009*; Springer: Berlin/Heidelberg, Germany, 2010; pp. 822–827.
9. Gao, J.L.; Zhang, M.X.; Lin, Y.L.; Qiu, C.C. Analysis of interaction mechanism of reinforced geomembrane and sandy sand interface. *Rock Sand Mech.* **2012**, *33*, 2465–2471. [CrossRef]
10. Gao, J.J.; Xu, H.; Qian, J.W. Settlement Behavior of Soft Subgrade Reinforced by Geogrid-Encased Stone Column and Geocell-Embedded Sand Cushion: A Numerical Analysis. *Adv. Civ. Eng.* **2022**, *2022*, 8874520. [CrossRef]
11. Zhang, M.X.; Zhang, S.L.; Huang, J. Behavior of interface between denti-strip geosynthetic reinforcements and sand under low surcharge. *Chin. J. Geotech. Eng.* **2007**, *29*, 1623–1629.